

# A Model Predictive Sliding Mode Control with Integral Action for Slip Suppression of Electric Vehicles

Tohru Kawabe

Faculty of Engineering, Information and Systems, University of Tsukuba, Tsukuba 305-8573, Japan

**Keywords:** Electric Vehicle, Slip Ratio, Robustness, Sliding Mode Control, Model Predictive Control.

**Abstract:** This paper proposes a new SMC (Sliding Mode Control) method with MPC (Model Predictive Control) algorithm for the slip suppression of EVs (Electric Vehicles). This method introducing the integral term with standard SMC gain, where the integral gain is optimized for each control period by solving an optimization problem based on the MPC algorithm to improve the acceleration performance and the energy consumption of EVs. Numerical simulation results are also included to demonstrate the effectiveness of the method.

## 1 INTRODUCTION

Over the past decades, the automobile population has been increasing rapidly in the developing countries, such as BRICs (Brazil, Russia, India and China) (Dargay et al., 2007). With the wide spread of automobiles all over the world, especially internal-combustion engine vehicles (ICEVs), the environment and energy problems: air pollution, global warming, oil resource exhaustion and so on, are going severely (Mamalis et al., 2013). As a countermeasure to these problems, the development of next-generation vehicles have been focused. EVs run on electricity only and they are zero emission and eco-friendly. So EVs have attracted great interests as a powerful solution against the problems mentioned above (Brown et al., 2010; Hirota et al., 2011; Tseng et al., 2013).

EVs are propelled by electric motors, using electrical energy stored in batteries or another energy storage devices. Electric motors have several advantages over ICEs (Internal-Combustion Engines):

- The input/output response is faster than for gasoline/diesel engines.
- The torque generated in the wheels can be detected relatively accurately
- Vehicles can be made smaller by using multiple motors placed closer to the wheels.

The travel distance per charge for EV has been increased through battery improvements and using regeneration brakes, and attention has been focused on improving motor performance. The above-mentioned

facts are viewed as relatively easy ways to improve maneuverability and stability of EVs.

It's, therefore, important to research and development to achieve high-performance EV traction control. Several methods have been proposed for the traction control (Fujii and Fujimoto, 2007) by using slip ratio of EVs, such as the method based on MFC (Model Following Control) in (Hori, 2000) We have been proposed MP-PID (Model Predictive Proportional-Integral-Derivative) method in (Kawabe et al., 2011) and MP-2DOF-PID method in (Kawabe, 2014).

These methods show good performances under the nominal conditions where the situations, for example, mass of vehicle, road condition, and so on, are not changed. To meet the high performance even variation happened in such conditions, it is significant to construct the robust control systems against the changing of situation. About this point, SMC performs good robustness against the uncertainties and nonlinearities of the systems.

However, for slip suppression with the conventional SMC (Slotine and Li, 1991; Eker and Akin, 2008), the control performance will get degradation due to the chattering which always occurs when switching the control inputs due to the structure of SMC. To overcome such disadvantages, the SMC method introducing the integral action with gain to design the sliding surface (SMC-I) has been proposed in (Li and Kawabe, 2013), where the integral gain is derived by trial and error. In order to get better control performance and save more energy for slip suppression of EVs with changing the mass of vehi-

cle and road condition, the optimal gain derived on-line is expected. Therefore, we have developed the Model Predictive Sliding Mode Control with Integral action (MP-SMC-I) (Li and Kawabe, 2014), which determines the integral gain adaptively at each step by MPC algorithm (Maciejowski, 2005). However, there are some room to improve the robust performance of this method. This paper, therefore, proposes the improved MP-SMC-I method. The simulation results are shown to verify the effectiveness of the proposed method.

## 2 ELECTRIC VEHICLE DYNAMICS

As a first step toward practical application, this paper restricts the vehicle motion to the longitudinal direction and uses direct motors for each wheel to simplify the one-wheel model to which the drive force is applied. In addition, braking was not considered this time with the subject of the study being limited to only when driving.

From fig. 1, the vehicle dynamical equations are expressed as eqs. (1) to (4).

$$M \frac{dV}{dt} = F_d(\lambda) - F_a - \frac{T_r}{r} \quad (1)$$

$$J \frac{d\omega}{dt} = T_m - rF_d(\lambda) - T_r \quad (2)$$

$$F_m = \frac{T_m}{r} \quad (3)$$

$$F_d = \mu(c, \lambda)N \quad (4)$$

Where  $M$  is the vehicle weight,  $V$  is the vehicle body velocity,  $F_d$  is the driving force,  $J$  is the wheel inertial moment,  $F_a$  is the resisting force from air resistance and other factors on the vehicle body,  $T_r$  is the frictional force against the tire rotation,  $\omega$  is the wheel angular velocity,  $T_m$  is the motor torque,  $F_m$  is the motor torque force conversion value,  $r$  is the wheel radius, and  $\lambda$  is the slip ratio.  $N$  is the normal tire force defined as  $N = Mg$  where  $g$  is the acceleration of gravity. The slip ratio is defined by eq. (5) from the wheel velocity ( $V_\omega$ ) and vehicle body velocity ( $V$ ).

$$\lambda = \begin{cases} \frac{V_\omega - V}{V_\omega} & \text{(accelerating)} \\ \frac{V - V_\omega}{V} & \text{(braking)} \end{cases} \quad (5)$$

$\lambda$  during accelerating can be shown by eq. (6) from fig. 1.

$$\lambda = \frac{r\omega - V}{r\omega} \quad (6)$$

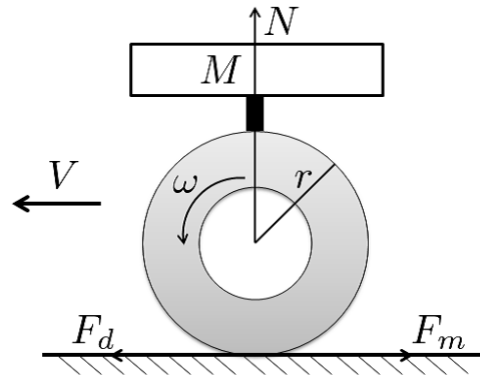


Figure 1: One-wheel car model.

The frictional forces that are generated between the road surface and the tires are the force generated in the longitudinal direction of the tires and the lateral force acting perpendicularly to the vehicle direction of travel, and both of these are expressed as a function of  $\lambda$ . The frictional force generated in the tire longitudinal direction is expressed as  $\mu$ , and the relationship between  $\mu$  and  $\lambda$  is shown by eq. (7) below, which is a formula called the Magic-Formula (Pacejka and Bakker, 1991) and which was approximated from the data obtained from testing.

$$\mu(\lambda) = -c_{road} \times 1.1 \times (e^{-35\lambda} - e^{-0.35\lambda}) \quad (7)$$

Where  $c_{road}$  is the coefficient used to determine the road condition and was found from testing to be approximately  $c_{road} = 0.8$  for general asphalt roads, approximately  $c_{road} = 0.5$  for general wet asphalt, and approximately  $c_{road} = 0.12$  for icy roads. For the various road conditions ( $0 < c < 1$ ), the  $\mu - \lambda$  surface is shown in fig. 2.

It shows how the friction coefficient  $\mu$  increases with slip ratio  $\lambda$  ( $0.1 < \lambda < 0.2$ ) where it attains the maximum value of the friction coefficient. As defined in eq. (4), the driving force also reaches the maximum

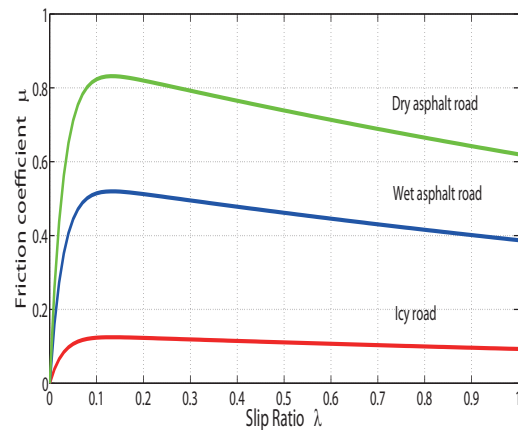


Figure 2:  $\mu - \lambda$  curve for road conditions.

value corresponding to the friction coefficient. However, the friction coefficient decreases to the minimum value where the wheel is completely skidding. Therefore, to attain the maximum value of driving force for slip suppression, it should be controlled the optimal value of slip ratio. the optimal value of  $\lambda$  is derived as follows. Choose the function  $\mu_c(\lambda)$  defined as

$$\mu_c(\lambda) = -1.1 \times (e^{-35\lambda} - e^{-0.35\lambda}). \quad (8)$$

By using eqs. (7) and (8), it can be rewritten as

$$\mu(c, \lambda) = c_{road} \cdot \mu_c(\lambda). \quad (9)$$

Evaluating the values of  $\lambda$  which maximize  $\mu(c, \lambda)$  for different  $c(c > 0)$ , means to seek the value of  $\lambda$  where the maximum value of the function  $\mu_c(\lambda)$  can be obtained. Then let

$$\frac{d}{d\lambda} \mu_c(\lambda) = 0 \quad (10)$$

and solving equation (10) gives

$$\lambda = \frac{\log 100}{35 - 0.35} \approx 0.13. \quad (11)$$

Thus, for the different road conditions, when  $\lambda \approx 0.13$  is satisfied, the maximum driving force can be gained. Namely, from eq. (7) and fig. 2, we find that regardless of the road condition (value of  $c$ ), the  $\lambda - \mu$  surface attains the largest value of  $\mu$  when  $\lambda$  is the optimal value 0.13.

### 3 MP-SMC WITH INTEGRAL ACTION DESIGN FOR SLIP SUPPRESSION

#### 3.1 SMC with Integral Action (SMC-I) Method

In this section, the previous proposed control strategy based on SMC with integral action (SMC-I) (Li and Kawabe, 2013) is explained. Without loss of generality, one wheel car model in fig. 1 is used for the design of the control law. The nonlinear system dynamics can be presented by a differential equation as

$$\dot{\lambda} = f + bT_m \quad (12)$$

where  $\lambda \in R$  is the state of the system representing the slip ratio of the driving wheel which is defined as eq. (5) for the case of acceleration,  $T_m$  is the control input.  $f$  describes the nonlinearity of system and  $b$  is the input gain, and they are all time-varying. Differentiating eq. (5) with respect to time gives

$$\dot{\lambda} = \frac{-\dot{V} + (1 - \lambda)\dot{V}_w}{V_w} \quad (13)$$

and substituting eqs. (1), (2) and (4) into eq. (13), the following equations can be attained,

$$f = -\frac{g}{V_w} \left[ 1 + (1 - \lambda) \frac{r^2 M}{J_w} \right] \mu(c, \lambda), \quad (14)$$

$$b = \frac{(1 - \lambda)r}{J_w V_w}. \quad (15)$$

The sliding mode controller is described to maintain the value of slip ratio  $\lambda$  at the desired value  $\lambda^*$ .

Referring to (Li and Kawabe, 2013), in order to reduce the undesired chattering effect for which it is possible to excite high frequency modes, and guarantee zero steady-state error, an integral action with gain has been introduced to the design of sliding surface. By adding an integral item to the difference between the actual and desired values of the slip ratio, the sliding surface function  $s$  is given by

$$s = \lambda_e + K_{in} \int_0^t \lambda_e(\tau) d\tau, \quad (16)$$

where  $\lambda_e$  is defined as  $\lambda_e = \lambda - \lambda^*$  and  $K_{in}$  is the integral gain,  $K_{in} > 0$ .

The sliding mode occurs when the state reaches the sliding surface defined by  $s = 0$ . The dynamics of sliding mode is governed by

$$\dot{s} = 0. \quad (17)$$

By using eqs. (12) to (17), the sliding mode control law is derived by adding a switching control input  $T_{msw}$  to the nominal equivalent control input  $T_{meq,n}$  as in (Li and Kawabe, 2013)

$$T_m = T_{meq,n} + T_{msw}, \quad (18)$$

$$T_{meq,n} = \frac{1}{b} [-f_n - K_{in}\lambda_e], \quad (19)$$

$$T_{msw} = \frac{1}{b} \left[ -K_{sat} \left( \frac{s}{\Phi} \right) \right], \quad (20)$$

$$\text{sat} \left( \frac{s}{\Phi} \right) = \begin{cases} -1 & s < -\Phi \\ \frac{s}{\Phi} & -\Phi \leq s \leq \Phi \\ 1 & s > \Phi \end{cases}, \quad (21)$$

where “ $_n$ ” is used to indicate the estimated model parameters.  $f_n$  is the estimation of  $f$  calculated by using the nominal values of vehicle mass  $M_n$  and road surface condition coefficient  $c_n$ .  $\Phi > 0$  is a design parameter which defines a small boundary layer around the sliding surface. The sliding gain  $K > 0$  is selected as

$$K = F + \eta \quad (22)$$

by defining Lyapunov candidate function in (Li and Kawabe, 2013), where  $F = |f - f_n|$  and  $\eta$  is a design parameter.

By using eqs. (18), (19), (20) and (22), the control law of SMC-I can be represented as

$$T_m = \frac{1}{b} \left[ -f_n - K_{in}\lambda_e - (F + \eta) \text{sat} \left( \frac{s}{\Phi} \right) \right]. \quad (23)$$

### 3.2 Improved Model Predictive SMC with Integral Action (MP-SMC-I) Method

In this section, we show the improved MP-SMC-I method. Although the MP-SMC-I method has been developed by us (Li and Kawabe, 2014), it has disadvantage to take time to calculate the predicted control input ( $\hat{T}_m$ ). Then we improved this point to propose new calculation method.

Generally, MPC algorithm is used to predict the future state behavior base on the discrete-time state space model (Maciejowski, 2005). The continuous time state space model for the slip ratio control represented by eq. (12) can not be dealt with in the same way. It is transformed to the discrete time state space model at sampling time  $t = kT$ ,  $T$  is the sampling period. The torque input is defined by

$$T_m(t) = T_m(kT), kT \leq t < (k+1)T. \quad (24)$$

For convenience, we will omit  $T$  in the following equations.

The controlled object of vehicle dynamics can be described as follows.

$$\lambda(k+1) = f_d(k, \lambda(k)) + b_d(k, \lambda(k))T_m(k) \quad (25)$$

where  $\lambda(k)$  is the state variable representing the slip ratio at time  $k$ .  $f_d(k, \lambda(k))$  describes the nonlinearity of the discrete time system,  $b_d(k, \lambda(k))$  is the input gain, and they are given by

$$f_d(k, \lambda(k)) = -\frac{g}{V_w(k)} \left\{ 1 + [1 - \lambda(k)] \frac{r^2 M}{J_w} \right\} \times \mu(c, \lambda(k)) \quad (26)$$

$$b_d(k, \lambda(k)) = \frac{[1 - \lambda(k)]r}{J_w V_w(k)}. \quad (27)$$

The control input  $T_m(t)$  given by eq. (23) can be rewritten as

$$T_m(k) = \frac{1}{b_d(k, \lambda(k))} \left\{ f_{dn}(k, \lambda(k)) - K_{in}(k) [\lambda(k) - \lambda^*] - [F_d(k, \lambda(k)) + \eta] \text{sat} \left( \frac{s(k, \lambda(k), K_{in}(k))}{\Phi} \right) \right\}$$

where  $\lambda^*$  is the reference slip ratio,  $\eta$  is the design parameter, and both of them are constants.  $f_{dn}(k, \lambda(k))$  is the estimation of  $f_d(k, \lambda(k))$  and is defined as

$$f_{dn}(k, \lambda(k)) = \frac{-g\mu(c_n, \lambda(k))}{V_w(k)} \left\{ 1 + [1 - \lambda(k)] \frac{r^2 M_n}{J_w} \right\}. \quad (28)$$

Now, we set current time to  $k$ . For a prediction horizon  $H_p$ , the predicted slip ratios  $\hat{\lambda}(k+i)$  for  $i = 1, \dots, H_p$  depend on the known values of current slip ratios, current torque input and future torque inputs. By using eq. (25), the predicted slip ratios can be represented as

$$\begin{aligned} \hat{\lambda}(k+H_p) &= f_d(k+H_p-1, \hat{\lambda}(k+H_p-1)) \\ &+ b_d(k+H_p-1, \hat{\lambda}(k+H_p-1)) \\ &\times \hat{T}_m(k+H_p-1) \end{aligned} \quad (29)$$

where  $\hat{T}_m(k+i)$ ,  $i = 0, \dots, H_p-1$  are predicted control inputs.  $\hat{T}_m(k+i)$  is given by

$$\hat{T}_m(k+i) = \frac{f_{dn}(k+i, \hat{\lambda}(k+i)) - K_{in} [\hat{\lambda}(k+i) - \lambda^*]}{b_d(k+i, \hat{\lambda}(k+i))} - \frac{[F_d(k+i, \hat{\lambda}(k+i)) + \eta] \text{sat} \left( \frac{s(k+i, \hat{\lambda}(k+i), K_{in})}{\Phi} \right)}{b_d(k+i, \hat{\lambda}(k+i))}.$$

Where

$$\begin{aligned} F_d(k, \lambda(k)) &= \frac{g}{|V_w(k, \lambda(k))|} \left| \mu(c_{max}, \lambda(k)) - \mu(c_n, \lambda(k)) \right| \\ &+ \frac{g(1 - \lambda(k))}{|V_w(k, \lambda(k))|} \frac{r^2}{J_w} \left| M_{max} \mu(c_{max}, \lambda(k)) - M_n \mu(c_n, \lambda(k)) \right| \end{aligned}$$

and where  $M_n$  is the estimated value of vehicle mass  $M$  and  $c_n$  is estimated for the viscous friction coefficient  $c$ . This calculation method of  $\hat{T}_m$  is improved method of previous our method (Li and Kawabe, 2014).

Here, we define the estimated values of these parameters respectively as the arithmetic mean of the value of the bounds.

$$c_n = \frac{c_{min} + c_{max}}{2} \quad (30)$$

$$M_n = \frac{M_{min} + M_{max}}{2}. \quad (31)$$

Actually, the mass of the car often changes with the number of passengers and the weight of luggage. Besides, the car has to always travel on various road surfaces. Then the ranges of variation in parameter  $c$  and parameter  $M$  are assumed to be defined as

$$c_{min} \leq c \leq c_{max} \quad (32)$$

$$M_{min} \leq M \leq M_{max}. \quad (33)$$

Here, the objective function  $J$  for deciding the value of  $K_{in}$  can be written as

$$J = \sum_{i=0}^{H_p-1} \left\{ q|\hat{\lambda}(k+i+1) - \lambda^*| + r|\hat{T}_m(k+i)| \right\} \quad (34)$$

where  $q, r$  are the positive weights. By using eqs. (29) and (30), both  $\hat{\lambda}$  and  $\hat{T}_m$  can be expressed by  $K_{in}$ , thus  $J$  can be represented by a function of  $K_{in}$ . Our aim is to find the parameter  $K_{in}$  that minimizes this objective function  $J(K_{in})$ . In a nutshell, the optimization problem is given by

$$\begin{aligned} & \min_{K_{in}} J(K_{in}) \\ & \text{s. t. [ Some constraint conditions} \\ & \quad \text{with input or output (if exist)} \end{aligned} \quad (35)$$

At time  $k$ , the optimal  $K_{in}(k)$  can be found by solving eq. (35) with some optimization method (here, a grid search method is made to the discretized  $K_{in}$ ) by MPC Algorithm. Once the optimal  $K_{in}(k)$  is determined, it is used as the continuous  $K_{in}(t)$  for  $kT \leq t < (k+1)T$ , then the continuous control input  $T_m(t)$  can be calculated by eq. (23). At the next sampling time  $k+1$ , the optimal  $K_{in}(k+1)$  is calculated as the previous step. At each sampling period, the same operation is repeated. Therefore, using the MP-SMC-I method could determine the optimal parameter  $K_{in}$  by solving the optimization problem.

## 4 NUMERICAL EXAMPLES

### 4.1 Simulation Settings

This section shows the numerical simulation results to demonstrate the effectiveness of the proposed method as shown in previous section. The performance of the proposed MP-SMC-I method is compared with that of no-control, SMC and SMC-I methods. In the simulation examples, the vehicle starts from rest and accelerates on icy road, wet asphalt road and dry asphalt road respectively with the parameters of dynamics shown in table 1. The maximum simulation time is set to 20[s] and the maximum velocity of the vehicle is 180[km/h].

Table 1: Parameters used in the simulations.

$J_w$ : Inertia of wheel	21.1 [kg/m <sup>2</sup> ]
$r$ : Radius of wheel	0.26 [m]
$\lambda^*$ : Desired slip ratio	0.13
$g$ : Acceleration of gravity	9.81 [m/s <sup>2</sup> ]

The SMC controller parameters  $\Phi, \eta$  as well as the integral gain  $K_{in}$  are listed in table 2 which are determined by trial and error.

Table 2: Controller settings

SMC	$\Phi = 1, \eta = 5$
SMC-I	$\Phi = 1, \eta = 5$ $K_{in} = 10$
MP-SMC-I	$\Phi = 1, \eta = 5$ $0 \leq K_{in} \leq 200, \Delta K_{in} = 1$ $q = 1.0 \times 10^8$ $r = 1.0$

In order to evaluate the energy consumption by the electric motor, we estimate the energy consumed for driving the wheel based on the following assumptions. Firstly, the electric power is all used to drive the wheel. Secondly, the power consumed by the vehicle is in proportional with the rotational energy due to the rotation of driven wheel. The rotational energy  $E_{rot}$  is defined by the rotational inertia of wheel  $J_w$  and the angular velocity  $w$  is given by

$$E_{rot} = \frac{1}{2} J_w w^2. \quad (36)$$

In the simulations, the total distance traveled is calculated by integrating the vehicle velocity from 0 to the simulation time  $t_{int}$  and is defined as

$$D_{dis} = \int_0^{t_{int}} V dt. \quad (37)$$

To learn how much the energy consumed with respect to the distance, the cost of the energy per distance (energy consumption rate) are also calculated.

### 4.2 Simulation Results

In order to verify the robustness of proposed MP-SMC-I with variation both in the mass of vehicle and road condition, the range of the uncertainties in the mass of vehicle  $M$  is [1000, 1400][kg] and the range of road condition coefficient  $c$  is [0.1, 0.9]. The nominal values used in the controller design taking the arithmetic mean of the edge values are  $M_n = 1200$ [kg],  $c_n = 0.5$ .

Furthermore, three road surfaces switch in the simulation by time as: an icy road ( $c = 0.12$ ) during [0, 0.45][s], another icy road ( $c = 0.20$ ) during [0.45, 8][s], a wet asphalt road ( $c = 0.50$ ) during [8, 9][s] and a dry asphalt road ( $c = 0.80$ ) during [9, 10][s].

As shown in fig. 3, the slip ratio can be suppressed to reference value 0.13 represented by black dot line accurately and rapidly regardless of the masses changing by 100[kg] from 1000[kg] to 1400[kg]. This implies that MP-SMC-I acts robustly to the variation in vehicle mass. It also makes a good transient performance at the switching spots on the road condition.

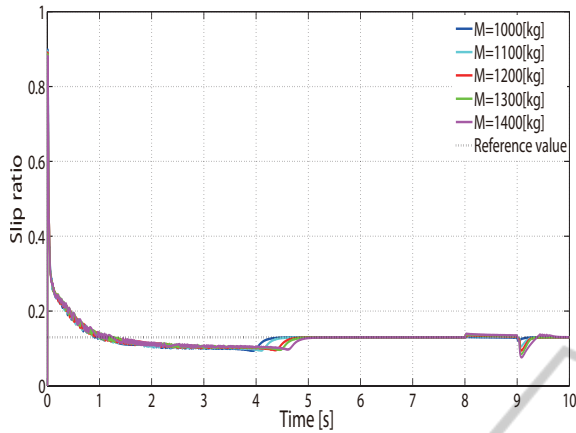
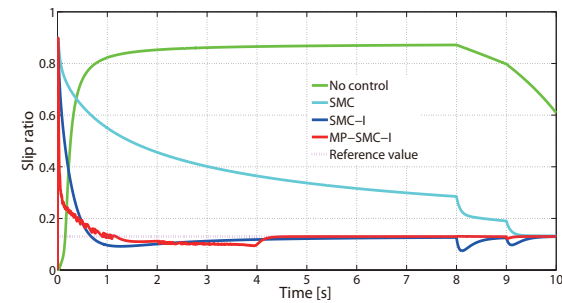
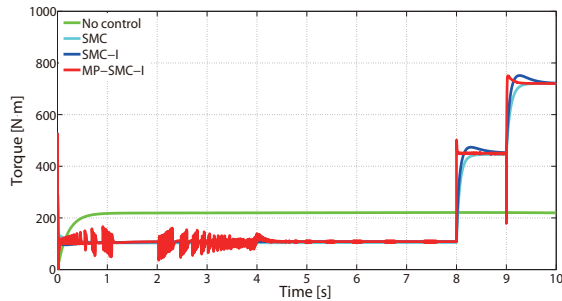


Figure 3: Time response of slip ratio with MP-SMC-I for different vehicle masses.

Next, we compared MP-SMC-I with the conventional SMC, SMC-I and no control. For saving of space, only results with the case of vehicle mass  $M$  assigned to 1000[kg] and 1400[kg] are limited to be shown below. From figs. 4 and 5 show the responses of slip ratio and motor torque under three different road conditions. The slip ratio by MP-SMC-I can be suppressed to the reference value more accurately and rapidly than SMC-I. When the road condition changes, the slip ratio by MP-SMC-I also keep an suitable transient performance, reducing the steady

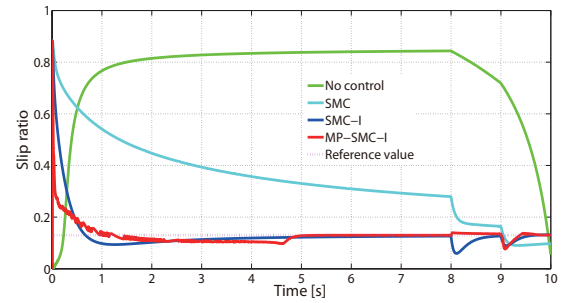


(a) Slip ratio

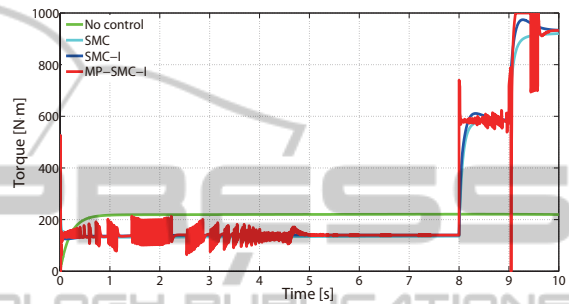


(b) Motor torque

Figure 4: Simulation results with No control, SMC, SMC-I and MP-SMC-I ( $M = 1000$ [kg]).



(a) Slip ratio



(b) Motor torque

Figure 5: Simulation results with No control, SMC, SMC-I and MP-SMC-I ( $M = 1400$ [kg]).

state error and rising time. The motor torque utilized by MP-SMC-I sufficiently to drive the wheel. The fluctuation in torque occurs at the time of road condition switching, which leads to  $K_{in}$  setting based on the prediction in the set prediction interval by the MPC algorithm.  $K_{in}$  is adjusted on-line for the optimum value from the objective function during the prediction interval when the road condition switches.

In fig. 6, the response of  $K_{in}$  varies sharply at the road condition switching spot because the tire grip margin changes, which leading to adjust  $K_{in}$  to achieve the sufficient driving force. Once the slip ratio deviates from the reference value,  $K_{in}$  is adjusted much based on MPC algorithm to get the appropriate force to drive the wheel to reach the reference value finally.

Then, to confirm the acceleration performance, we compare MP-SMC-I with SMC-I, SMC and No control. As shown in fig. 7, the curve of the vehicle velocity with MP-SMC-I coincides with the one with SMC-I almost. But we can see that the vehicle with MP-SMC-I represented by the red curve achieves the maximum driving force for the best acceleration during the whole simulation time.

Finally, table 3 show the results of the energy consumed  $E_r$ , the total distance  $D_d$  and the energy consumption rate  $E_p$  for different mass of vehicle. We can see that the energy consumption rate with MP-

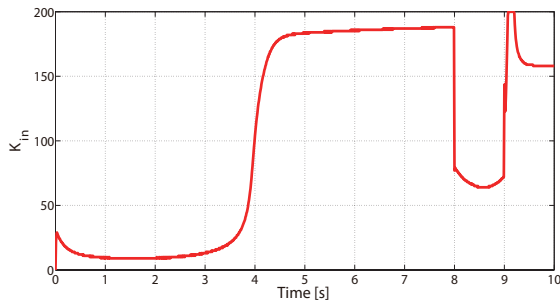
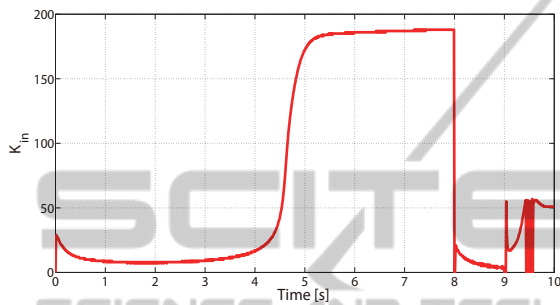

(i)  $M = 1000[\text{kg}]$ 

(ii)  $M = 1400[\text{kg}]$ 

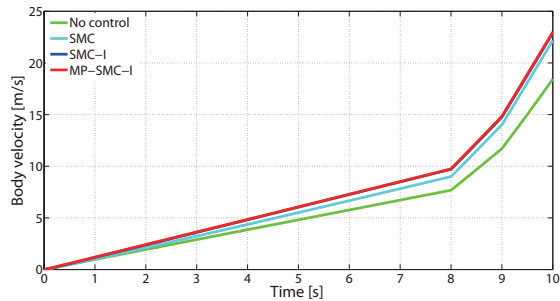
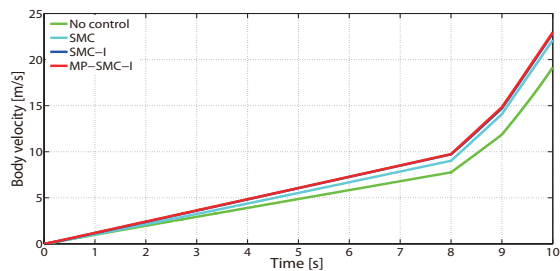
Figure 6: Time response of  $K_{in}$  for MP-SMC-I.

(i)  $M = 1000[\text{kg}]$ 

(ii)  $M = 1400[\text{kg}]$ 

Figure 7: Time response of body velocity with No control, SMC, SMC-I and MP-SMC-I.

SMC-I is nearly as much as the one with SMC-I, but the total distance is longer than SMC-I. This indicates that the vehicle with MP-SMC-I achieve a better acceleration performance. As the same result as the pre-

Table 3: Results of energy consumption rate with No control, SMC, SMC-I and MP-SMC-I.

(i) ( $M = 1000[\text{kg}]$ )

	$E_r$ [Wh]	$D_d$ [m]	$E_p$ [Wh/km]
No control	80.34	55.52	1447
SMC	28.30	64.82	437
SMC-I	28.11	69.58	404
MP-SMC-I	28.64	70.03	409

(ii) ( $M = 1400[\text{kg}]$ )

	$E_r$ [Wh]	$D_d$ [m]	$E_p$ [Wh/km]
No control	62.75	56.33	1114
SMC	35.10	64.98	540
SMC-I	36.22	69.54	521
MP-SMC-I	36.90	70.02	527

vious chapter described, due to the mass increasing caused much energy cost that the EV should be made more light without detriment to performance.

## 5 CONCLUSIONS

In this paper, the improved MP-SMC-I method has been proposed for robust slip suppression problem of EVs. We can verified that the the proposed method shows good robust performance against the changing of road condition and vehicle mass by numerical simulations. Also this method shows the good energy consumption performance. At the present stage, effectiveness of the proposed method is only confirmed by numerical simulations. Next step, therefore, is to realize the real system using the proposed method and to proof the advantage of such system by real experiments. Furthermore, in future work, the suitability of the proposed method must be studied not only for the slip suppression addressed by this paper but also for overall driving including during braking. Even for this issue, however, the basic framework of the method can be expanded relatively easily to the foundation for making practical EVs with high performance and safety traction control systems.

## ACKNOWLEDGEMENTS

This research was partially supported by Grant-in-Aid for Scientific Research (C) (Grant number: 24560538; Tohru Kawabe; 2012-2014) from the Ministry of Education, Culture, Sports, Science and Technology of Japan.

## REFERENCES

- Brown, S., Pyke, D., and Steenhof, P. (2010). Electric vehicles: The role and importance of standards in an emerging market. *Energy Policy*, 38(7):3797–3806.
- Dargay, J., Gately, D., and Sommer, M. (2007). Vehicle ownership and income growth, worldwide: 1960-2030. *The Energy Journal*, 28(4):143–170.
- Eker, I. and Akinal, A. (2008). Sliding mode control with integral augmented sliding surface: Design and experimental application to an electromechanical system. *Electrical Engineering*, 90:189–197.
- Fujii, K. and Fujimoto, H. (2007). Slip ratio control based on wheel control without detection of vehiclespeed for electric vehicle. *IEEJ Technical Meeting Record*, VT-07-05:27–32.
- Hirota, T., Ueda, M., and Futami, T. (2011). Activities of electric vehicles and prospect for future mobility. *Journal of The Society of Instrument and Control Engineering*, 50:165–170.
- Hori, Y. (2000). Simulation of mfc-based adhesion control of 4wd electric vehicle. *IEEJ Record of Industrial Measurement and Control*, pages IIC-00–12.
- Kawabe, T. (2014). Model predictive 2dof pid control for slip suppression of electric vehicles. *Proceedings of 11th International Conference on Informatics in Control, Automation and Robotics*, 2:12–19.
- Kawabe, T., Kogure, Y., Nakamura, K., Morikawa, K., and Arikawa, K. (2011). Traction control of electric vehicle by model predictive pid controller. *Transaction of JSME Series C*, 77(781):3375–3385.
- Li, S. and Kawabe, T. (2013). Slip suppression of electric vehicles using sliding mode control method. *International Journal of Intelligent Control and Automation*, 4(3):327–334.
- Li, S. and Kawabe, T. (2014). Slip suppression of electric vehicles using sliding mode control based on mpc algorithm. *International Journal of Engineering and Industries*, 5(4):11–23.
- Maciejowski, J. (2005). *Predictive Control with Constraints*. Tokyo Denki University Press (Trans. by Adachi, S. and Kanno, M.) (in Japanese).
- Mamalis, A., Spentzas, K., and Mamali, A. (2013). The impact of automotive industry and its supply chain to climate change: Somme techno-economic aspects. *European Transport Research Review*, 5(1):1–10.
- Pacejka, H. and Bakker, E. (1991). The magic formula tire model. *Vehicle system dynamics*, 21:1–18.
- Slotine, J. and Li, W. (1991). *Applied nonlinear control*. Prentice-Hall.
- Tseng, H., Wu, J., and Liu, X. (2013). Affordability of electric vehicle for a sustainable transport system: An economic and environmental analysis. *Energy Policy*, 61:441–447.